NANOFABRICATION OF CHALCOGENIDE GLASS FOR INFRARED SENSORS

Le Wei, Liang Dong*, and Meng Lu*
Iowa State University, USA

ABSTRACT

This paper reports a novel nanofabrication approach that combines imprint and silver doping lithography (iSDL) to generate nanoscale patterns in chalcogenide (ChG) thin films. The iSDL approach is capable of controlling the photodoping of silver in amorphous ChG with a high spatial precision. The ChG nanophotonic devices with one-dimensional (1D) and two-dimensional (2D) periodic structures were fabricated and characterized.

KEYWORDS

Chalcogenide, Imprint lithography, Nanophotonics, Silver doping.

INTRODUCTION

Featured with the low material loss in the infrared region, chalcogenide (ChG) has been exploited for a variety of photonic applications [1-5]. For example, ChG-based high-Q optical resonators have been demonstrated as refractometric sensors. In addition, the strong nonlinearity of ChG materials can be used for nonlinear applications, such as the second-harmonic and supercontinuum generations [6, 7]. In this regard, nanostructured ChG devices, which can enhance the interaction of light and ChG materials, are particular interesting.

ChG thin films can be selectively doped by silver when it is exposed to light with the photon energy larger than the bandgap of the ChG material[8]. The photodoping process has been adopted as a lithography approach, where the ChG film functions as the inorganic photoresist. The silver-doped and undoped ChG materials exhibit different solubilities in ammonia-based developers. The inorganic ChG resist can support patterns with high-resolution and high aspect ratio [9, 10]. To create nanoscale patterns, ChG thin film can also be silver doped by the direct writing using electron beam. However, the electron beam lithography is too slow and expensive to fabricate nanoscale patterns over a large surface area. On the other hand, to facilitate the fabrication of subwavelength structures, a number of nanoimprint lithography processes have been demonstrated [11] during the past two decades. The nanoimprinting lithography methods enable inexpensive fabrication of nanoscale patterns in imprint resist over large surface area.

Here, we present a new nanofabrication approach that leverages the advantages of both imprint and silver doping lithographies (iSDL) to generate subwavelength patterns in ChG film with a low cost, high throughput, and high spatial resolution. The iSDL method only requires an imprint mold coated with a thin layer of silver

and a light source with the wavelength below 500 nm. The iSDL method is capable of generate silver-doped ChG structures with the resolution smaller than the diffraction limit.

UNDERLYING PRINCIPLE

ChG materials, such as As₂S₃, have been investigated for the light-driven doping of metals, also known as photodoping or photodissolution [12-14]. As illustrated in Fig. 1, the thin layer of silver is deposited on the surface of the ChG thin film and the silver layer is selectively exposed by the light source. When the photoenergy is larger than the band gap of the ChG material, the photon can be absorbed, and an electron-hole pair is generated. By capturing holes, silver atoms are oxidized and become silver ions. Meanwhile, the electrons are trapped by chalcogen atoms. The built-in electrostatic force facilitates the diffusion of silver ions. When the silver ions recombine with the electrons, they are reduced and doped in the ChG material [13].

The iSDL process is based on the photodoping phenomenon and uses the imprint lithography to control the distribution of silver dopant source. To perform iSDL, a polymethylsiloxane (PDMS) mold, which carries the desired nanoscale pattern, is coated with a thin layer (20 nm) of silver and attached to the ChG film. The excitation light passes through the transparent PDMS mold to dope the silver into the ChG film. The resolution of the iSDL is determined by the pattern resolution on the PDMS mold, rather than the wavelength of the excitation light.

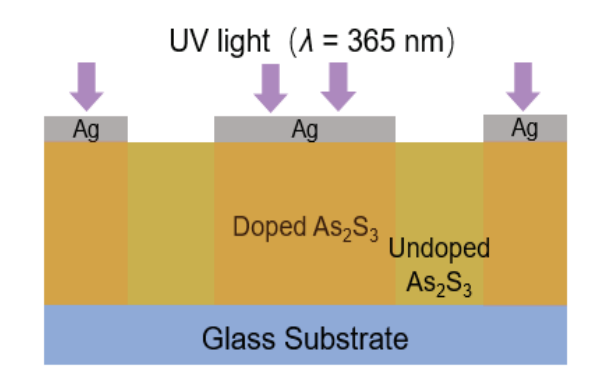


Figure 1. Mechanism of photodoping of silver in ChG.

DESIGN

To demonstrate the strengths of the iSDL approach, we fabricated several 1D and 2D ChG gratings. Figure 2 illustrates three different types of ChG nanostructures fabricated on a glass substrate. For the 1D structures, gratings with two different periods of $\Lambda_{\rm 1D} = 550$ nm and 179 nm, were tested. Fig. 2(b) and 2(c) show the 2D ChG

nano-hole and nano-dome structures, respectively.

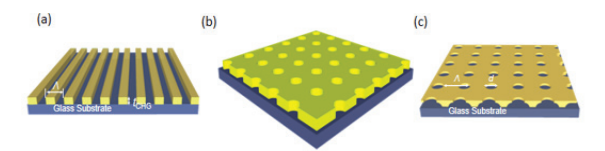


Figure 2. (a) Schematic of the 1D silver-doped ChG grating structure. (b) Schematic of the 2D silver-doped ChG grating. (c) Schematic of the 2D array of ChG nanodomes.

FABRICATION

Fig. 3 illustrates the major steps of the iSDL process. The As_2S_3 thin film was coated on a glass substrate using e-beam evaporation. The PDMS mold carrying the target pattern was coated with a thin layer of silver ($t_{Ag} < 20$ nm). Then, the silver-coated PDMS was attached to the As_2S_3 film and exposed under ultraviolet (UV) light (365 nm). During exposure, the silver layer on the top surface of the PDMS mold was in direct contact with the As_2S_3 film and can diffuse into the As_2S_3 film. In contrast, the silver coating in the grating trenches or the bottom of the nanoholes was not doped into the As_2S_3 film.

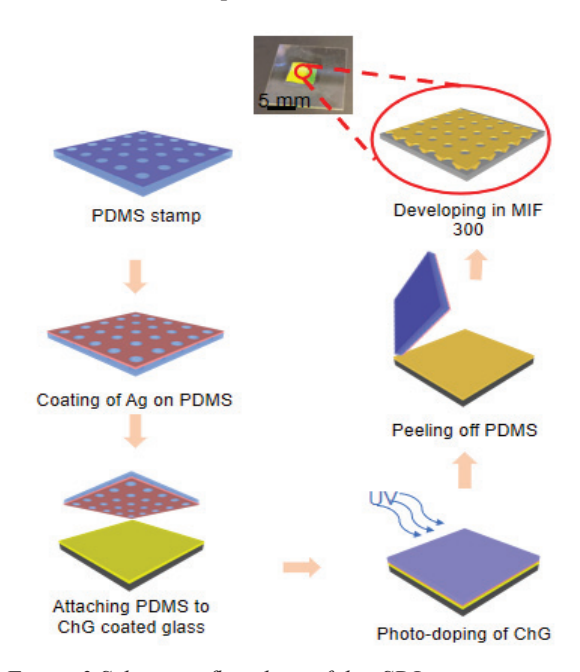


Figure 3 Schematic flowchart of the iSDL process.

The intensity and dose of the UV exposure were controlled in order to diffuse silver ions to the target region. After exposure, the As₂S₃ sample was developed in the ammonium-based developer (AZ MIF 300). The undoped ChG was quickly dissolved in the developer. By and large, the iSDL controls the horizontal and vertical distribution of silver ions in the ChG film using the preformed pattern on the PDMS stamp and the UV exposure, respectively. In contrast to conventional nanoimprint lithography [11] the iSDL is free of any residue layer and can offer highly uniform patterns.

RESULTS AND DISCUSSIONS

Fabrication Results

The fabricated 1D ChG gratings were characterized using a scanning electron microscopy (SEM). The period and depth of the As₂S₃ grating shown in Fig. 4(a) are λ_{1D} = 550 nm and t_{ChG} = 300 nm, respectively. Fig. 4(b) shows the As₂S₃ grating with the period as small as λ_{1d} = 179 nm and the minimum feature size of 90 nm. Fig. 5 shows the SEM images of 2D As₂S₃ gratings with Λ_{2D} = 700 nm and 300 nm, receptively.

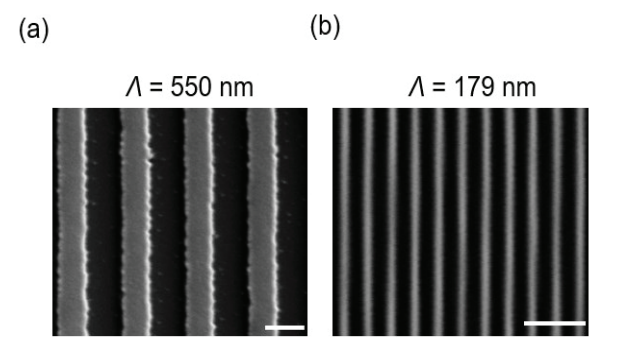


Figure 4. SEM images of the fabricated ChG 1D gratings with different periods. Scale bar: 500 nm

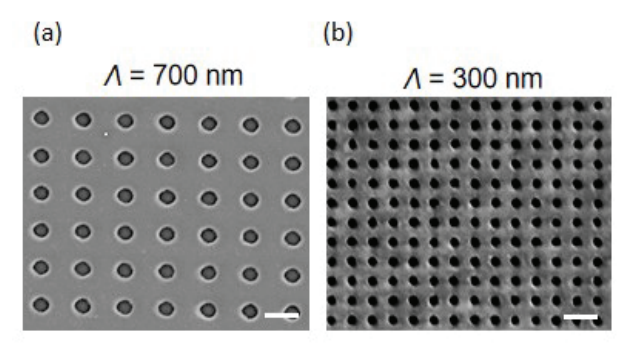


Figure 5. SEM images of the fabricated ChG 2D gratings with different periods. Scale bar: 500 nm

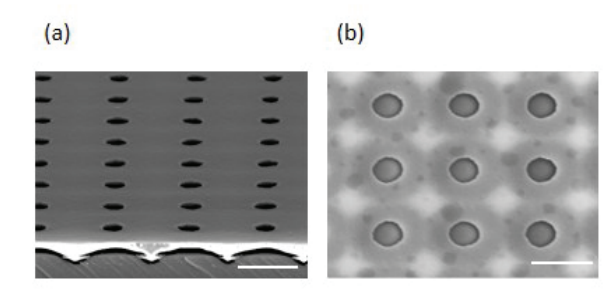


Figure 6. SEM images of the fabricated ChG 2D nanodomes top and side view. Scale bar: 500nm

We also fabricated the As_2S_3 nano-dome structure by controlling the lateral diffusion of silver in the As_2S_3 film. The isotropic development of undoped As_2S_3 under the thin layer of silver-doped As_2S_3 resulted in the nano-dome array with the period of $\varLambda_{2D} = 700$ nm.

Optical Characteristics

The 2D As₂S₃ grating slab on a glass substrate can support the leaky mode resonances [15]. Fig. 7 shows the optical setup we used to measure the transmissions of the sample. The emission of broadband light is collimated and illuminates the sample. The transmitted light is collected and analyzed by a near-infrared spectrometer (StellarNet Inc.). The angle of incidence (θ_i) can be tuned by rotating the sample.

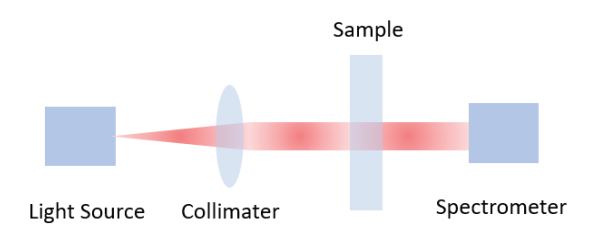


Figure 7. Schematic diagram of the transmissions measurement setup.

The transmission characteristics of the fabricated device with $\Lambda_{2D}=700$ nm (shown in Fig. 6) were measured and simulated using an electromagnetic simulation tool. The results are compared in Fig. 8. As can be seen, the measurement and simulation results agree well. The device exhibits a leaky mode resonance at $\lambda_r=1040$ nm, which is manifested as the transmission dip. Due to the diverging of the incidence light beam, the linewidth of the resonant peak is slightly wider than the linewidth obtained using simulation.

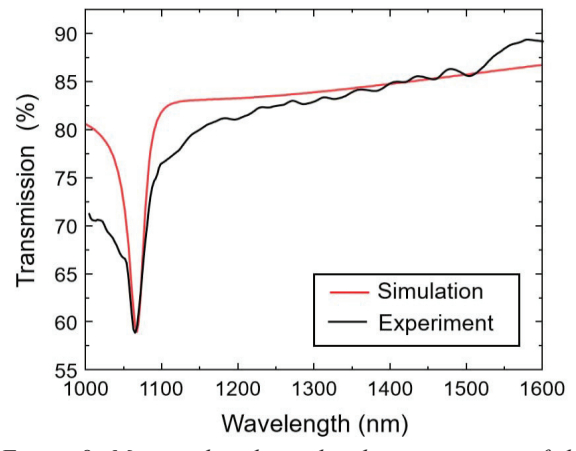


Figure 8. Measured and simulated transmittance of the 2D ChG nano-dome array shown in Fig. 6. The simulation was performed using the rigorous coupledwave analysis.

The transmittance of the As_2S_3 grating depends on the angle of incidence. To investigate the angle dependence of the leaky mode resonance, we mounted the sample on a rotation stage. The transmission spectra were measured at $\theta_i = 0^\circ$, 2° , 4° , 6° , and 8° . As shown in Fig. 9, when the incident angle was increased, the resonant mode at $\lambda_r = 1040$ nm split into two resonances. These two resonant modes shifted towards the longer and shorter wavelengths. At $\theta_i = 8$ of the resonant modes located at

1010 nm and 1100 nm, respectively.

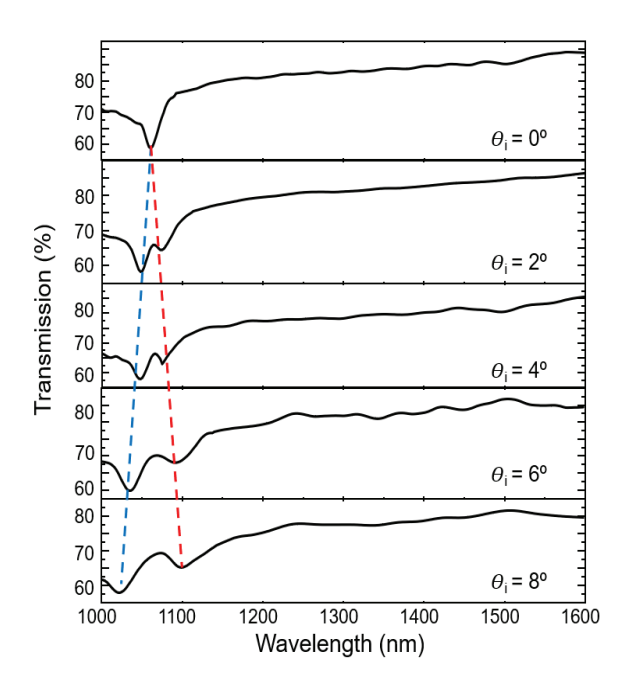


Figure 9. Transmission spectra as a function of the incident angle for the 2D ChG array of nano-domes.

CONCLUSION

We developed and demonstrated the iSDL approach for the fabrication of ChG-based nanophotonic devices. The 1D and 2D periodic structures with different periods were fabricated by doping of silver provided by the PDMS molds. The results show that the iSDL approach can produce high quality sub-wavelength structures with low cost, large surface area, and high throughput. As an example, we characterized the leaky mode resonance supported by the 2D ChG array of nano-domes. The silvedoped ChG device exhibits the resonant modes in the near infrared wavelength range. This technology will find various applications in infrared sensing [16][17] and communications.

ACKNOWLEDGEMENTS

This research was supported in part by the National Science Foundation (NSF) through the grant numbers ECCS-1711839 and ECCS-1653673.

REFERENCES

- [1] L. Li, et al. Integrated flexible chalcogenide glass photonic devices. *Nature Photonics*, 8.8 (2014): 643-649
- [2] V.A. Kamensky, et al. High-power As-S glass fiber delivery instrument for pulse YAG: Er laser radiation. Applied Optics, 37.24 (1998): 5596-5599.
- [3] X.H. Zhang, et al. Evaluation of glass fibers from the Ga-Ge-Sb-Se system for infrared applications. *Optical Materials*, 25.1 (2004): 85-89.

- [4] A. Faraon, et al. Local tuning of photonic crystal cavities using chalcogenide glasses. *Applied Physics Letters*, 92.4 (2008): 043123
- [5] M.L. Anne, et al. Chalcogenide Glass Optical Waveguides for Infrared Biosensing. Sensors, 9.9 (2009): 7398-7411.
- [6] M. Malinowski, et al. Amplified octave-spanning supercontinuum from chalcogenide waveguides for second-harmonic generation. 30th Annual Conference of the IEEE Photonics Society (2017): 261-262.
- [7] N.W. Rosemann, et al. Organotetrel Chalcogenide Clusters: Between Strong Second-Harmonic and White-Light Continuum Generation. *Journal of the American Chemical Society*, 138.50 (2016): 16224-16227.
- [8] M. Frumar, et al. Ag doped chalcogenide glasses and their applications. *Current Opinion in Solid* State & Materials Science, 7.2 (2003): 117-126.
- [9] A. Kovalskiy, et al. Chalcogenide glass e-beam and photoresists for ultrathin grayscale patterning. *Journal of Micro-Nanolithography Mems and Moems*, 8.4 (2009): 043012
- [10] A. Kovalskiy, et al. Development of chalcogenide glass photoresists for gray scale lithography. *Journal of Non-Crystalline Solids*, 352.6-7 (2006): 589-594.
- [11] S.H. Ahn, et al. Large-Area Roll-to-Roll and Roll-to-Plate Nanoimprint Lithography: A Step toward High-Throughput Application of Continuous Nanoimprinting. Acs Nano, 3.8 (2009): 2304-2310.
- [12] R. Elghrandi, et al. Silver Photodissolution in Amorphous-Chalcogenide Thin-Films. *Thin Solid Films*, 218.1-2 (1992): 259-273.
- [13] A. Lorinczi, et al. Silver doped As2S3 chalcogenide films: A diffusion study. *Physica Status Solidi C: Current Topics in Solid State Physics*, 8.9 (2011): 2617-2620.
- [14] J. Calas, et al. Photodissolution Profile of Silver in Amorphous-Chalcogenide Gesex Thin-Films.

 Nuclear Instruments & Methods in Physics Research Section B-Beam Interactions with Materials and Atoms, 63.4 (1992): 462-472.
- [15] N. Ganesh, et al. Leaky-mode assisted fluorescence extraction: application to fluorescence enhancement biosensors. *Optics Express*, 16.26 (2008): 21626-21640.
- [16] D. Liang, et al. Characterization of uncooled poly SiGe microbolometer for infrared detection. *Chinese Physics Letters*, 20.5 (2003): 770-773.
- [17] L. Dong, et al. Design and fabrication of single-chip a-Si TFT-based uncooled infrared sensors. *Sensors and Actuators A: Physical*, 116.2 (2004): 257-263.

CONTACT

- *Liang Dong, <u>ldong@iastate.edu</u>
- *Meng Lu, menglu@iastate.edu